Carbohydrate Polymers 101 (2014) 533–543

Contents lists available at ScienceDirect

Carbohydrate Polymers

journal homepage: www.elsevier.com/locate/carbpol

Protective effect of *Millettia pulchra* polysaccharide on cognitive impairment induced by D-galactose in mice

Xing Lin[a,1], Zhongshi Huang[b,1], Xiaoyu Chen[a], Yanping Rong[a], Shijun Zhang[a], Yang Jiao[a], Quanfang Huang[a], Renbin Huang[a,*]

[a] Guangxi Medical University, Nanning, Guangxi 530021, China
[b] Youjiang Medical College for Nationalities, Baise, Guangxi 533000, China

ARTICLE INFO

Article history:
Received 26 May 2013
Received in revised form 7 August 2013
Accepted 14 September 2013
Available online 23 September 2013

Keywords:
Polysaccharide
Millettia pulchra
Cognitive impairment
D-Galactose

ABSTRACT

A polysaccharide (PMP) was isolated from *Millettia pulchra* and purified by DEAE-cellulose and Sephadex G-75 chromatography. The results showed that PMP was composed of D-glucose and D-arabinose in a molar ratio of 90.79% and 9.21%, with an average molecular weight of about 14,301 Da. Furthermore, the effect of PMP on cognitive impairment induced by D-galactose in mice was evaluated. Treatment with PMP significantly reversed D-galactose-induced learning and memory impairments, as measured by behavioral tests. One of the potential mechanisms of this action was to reduce oxidative stress and suppress inflammatory responses. Furthermore, our results also showed that PMP markedly reduced the content and deposition of β-amyloid peptide, improved the dysfunction of synaptic plasticity, increased the levels of acetylcholine, but decreased cholinesterase activity. These results suggest that PMP exerts an effective protection against D-galactose-induced cognitive impairment, and PMP may be a major bioactive ingredient in *M. pulchra*.

1. Introduction

Memory decline is characteristic of aging and age-related neurodegenerative disorders which lead to a progressive loss of cognitive function, especially in spatial memory (Zhang, Jiang, Li, Hao, & An, 2007). It has been proposed that formation of reactive oxygen species (ROS) is an important step leading to neuronal death in a variety of age-related neurodegenerative disorders (Castegna et al., 2002; De Iuliis, Grigoletto, Recchia, Giusti, & Arslan, 2005). ROS oxidizes various biological macromolecules, thereby disturbing homeostatics within the neuron and ultimately resulting in cell death. D-Galactose (D-gal) can cause the accumulation of ROS, or stimulate free radical production indirectly by the formation of advanced glycation endprodcts (AGE) in vivo, finally resulting in oxidative stress (Zhang, Li, Cui, & Zuo, 2005). D-Gal can also impair neurogenesis in the dentate gyrus, a process similar to natural aging in mice (Cui et al., 2006). Therefore, D-gal-induced senescent mouse is a good model for studying age-related damage in brain (Wei et al., 2005).

Drugs isolated from traditional medicinal plants may provide a promising therapy on brain injuries caused by oxidative stress. An example of a traditional herb that is often used in popular folk medicine in the Guangxi Zhuang Autonomous Region of China is *Millettia pulchra* (Leguminosae *M. pulchra* Kurz), which is often used as an anti-aging and memory improving agent (Huang, Jiao, Zhang, & Huang, 2008). The active components of *M. pulchra* primarily consist of polysaccharides, amino acids, glycosides and flavonoids (Li, 2011). Our previous studies, which examined the crude polysaccharides content from *M. pulchra* (Huang et al., 2009), demonstrated that treatment with the *M. pulchra* crude polysaccharides significantly increased neurotransmitter content in the brain, promoted the metabolism of free radicals, and improved cognitive abilities in animal dementia models (Huang, Lin, et al., 2008; Huang, Xie, et al., 2008). Furthermore, the crude polysaccharides significantly reduced the over-expression of β-amyloid (Aβ), β-site amyloid precursor protein cleaving enzyme (BACE) and β-amyloid precursor protein (APP) in senescence-accelerated mouse prone 8 mice in a dose-dependent manner (Huang et al., 2009). However, the active ingredients in the crude polysaccharides content and the mechanisms by which these active ingredients ameliorate cognitive deterioration remain elusive. Extracting the bioactive fractions from the crude polysaccharides is a valid approach, which allows for the pharmacological assessment of substrates and effects. Preliminary screening of several fractions from the crude polysaccharides indicated that a polysaccharide named PMP, with composed of arabinosyl and glucosyl residue, may be an active fraction; this fraction showed good neuroprotective action and was a relatively clean ingredient.

* Corresponding author. Tel.: +86 0771 5339805.
E-mail address: huangrenbin518@163.com (R. Huang).
[1] These authors contributed equally to this work.

0144-8617/$ – see front matter © 2013 Elsevier Ltd. All rights reserved.
http://dx.doi.org/10.1016/j.carbpol.2013.09.037

Based on the preliminary screening, we hypothesized that PMP could protect the brain from cognitive impairment. In the present study, we investigated the effect of PMP on cognitive impairment and oxidative injury induced by D-galactose in mice. The molecular mechanisms involved in the prevention of learning and spatial memory loss were also studied.

2. Materials and methods

2.1. Drugs and chemicals

M. pulchra (Leguminosae *M. pulchra* Kurz) was purchased from Nanning Qianjinzi Chinese Pharmaceutical Co. Ltd. (Nanning, China). A voucher specimen (YLS20110312619) was identified by Professor Quanfang Huang in the Department of Pharmacognosy, The First Affiliated Hospital of Guangxi University of Chinese Medicine and deposited in the herbarium of Department of Pharmacology of Guangxi Medical University.

D-Galactose (D-gal) was purchased from Sino-American Biotechnology Co., Ltd. (Luoyang, China), and dissolved in physiological saline. Huperzine A was purchased from Yuzhong Drug Manufactory (Henan, China). Malondialdehyde (MDA), superoxide dismutase (SOD), glutathione (GSH), nitric oxide (NO), glutathione peroxidase (GPX), neuronal nitric oxide synthase (nNOS) and total NOS kits were obtained from Nanjing Jiancheng Bioengineering Research Institute (Nanjing, China).

2.2. Preparation of PMP

2.2.1. Preparation of crude polysaccharides from M. pulchra

Dry, sliced *M. pulchra* (1.5 kg) was extracted with 12 L of water for 2 h at 95 °C three times. The combined extracts were filtered, concentrated and centrifuged, and then the supernatant was treated with 3 volumes of ethanol at 4 °C overnight. The precipitate was separated by filtration, washed exhaustively with 95% ethanol, and then dissolved in deionized water and dialyzed using cellulose sacks (8000–10,000 D, Sigma) against flowing water for 48 h. The non-dialyzed portion was precipitated again with three volumes of ethanol overnight. The resulting precipitate was filtrated and washed exhaustively first with anhydrous ethanol, then with acetone and finally with anhydrous ether; 102.86 g of crude polysaccharides was obtained.

2.2.2. Anion-exchange chromatographic method

The crude polysaccharides (100 mg) were dissolved in distilled water and filtered through a membrane (0.45 μm, Nucleopore). Then the solution was applied to a DEAE-Sepharose fast-flow column (3 cm × 45 cm) pre-equilibrated with 20 mM Tris–HCl buffer (pH 7.8). Fractions were prepared in a stepwise elution with increased concentration of NaCl (0.1–1 M) solution at a flow rate of 1.0 ml/min, and with collection of 5 ml for each tube. The polysaccharide content in each fraction was detected by phenol–sulphuric acid method (Zhang et al., 2007). The appropriate fractions were concentrated, dialyzed against water, and finally lyophilized.

2.2.3. Gel-filtration chromatography

Size-exclusion chromatography of the purified polysaccharide was performed on Sephadex G-75 (20 × 600 mm), and 0.1 M NaCl was used as eluant. The major polysaccharides fractions were collected with a fraction collector, then dialyzed with water, and lyophilized to give a polysaccharide named PMP, which was used in subsequent analyses.

2.2.4. Physicochemical property of PMP

Total carbohydrate content of PMP was determined by phenol-sulfuric acid colorimetric method using D-glucose as standard (Taylor, 1995). Protein content was quantified according to the method of Bradford (1976), using bovine serum albumin as standard reference material. Sulphate content was measured from about 10 mg of samples after 2 mol/l HCl hydrolysis (2 h at 100 °C), as described elsewhere (Kawai, Seno, & Anno, 1969). Uronic acid content was estimated by m-hydroxydiphenyl assay using glucuronic acid as the standard (Filisetti-Cozzi & Carpita, 1991).

2.2.5. Molecular weight determination

The homogeneity and molecular weight of PMP were determined by high-performance gel-permeation chromatography (HPGPC). The sample solution (20 μl of 0.5%) was applied to Agilent 1100 HPLC system equipped with a Dhpak SB-803 HQ (8.0 mm × 300 mm), eluted with 0.05 M Na_2SO_4 solution at a flow rate of 0.5 ml/min and detected by a RID-10A refractive index detector. The columns were calibrated with T-series dextran (T-200, T-70, T-40, T-20 and T-10) and glucose as standards. The molecular weight of PMP was estimated by the calibration curve.

2.2.6. Polysaccharide hydrolysis with acid and monosaccharides derivative

The PMP (10 mg) was hydrolysed with 2 M trifluoroacetic acid (TFA) (10 ml) for 8 h at 100 °C in a sealed glass tube. The excess acid was completely removed at 70 °C by a steady stream of nitrogen, and the hydrolysed products were used for the preparation of its derivative. The reaction was carried out by mixing 10 mg of hydrolysed products and 5 ml 0.5 M NaOH, and then 6 ml 0.5 M 1-phenyl-3-methyl-5-pyrazolone methanol solution were added followed by incubation at 70 °C water bath for 30 min. Subsequently the tube was cooled down to room temperature, and 0.5 M HCl was added to neutralize solution pH to 7. Finally, the solution was extracted with 20 ml $CHCl_3$ twice. The extract was centrifuged (3000 rpm, 15 min), the supernatant was collected and the derivatives of the sugars were performed on HPCE. As references, the following neutral sugars were derived and analyzed: L-rhamnose, D-arabinose, D-xylose, D-glucose and D-galactose.

2.2.7. High-performance capillary electrophoresis (HPCE) analysis

HPCE was performed on an uncoated fused-silica capillary tube (50 μm × 70 cm) at 25 °C using 75 mM sodium tetraborate buffer (pH 9.5) as solvent, the absorbance was detected at 254 nm. Before each run, the capillary tube was washed by methanol (5 min), double distilled water (2 min), 0.1 M HCl (5 min), double distilled water (2 min), 0.1 M NaOH (10 min), double distilled water (2 min), and conditioned with the operating buffer for 10 min. The samples to be analyzed were injected automatically, using the low pressure injection mode (0.5 psi), in which the sample is pressurized for 5 s. The injection volume can be calculated with the Poiseuille equation, as proposed by the manufacturer, giving an estimated volume of 6 nl/s of injection time. Electrophoresis was performed at 15 kV using normal polarity. Peak areas were recorded and calculated using the Beckman software system.

2.3. Animals and treatment

Male Kunming mice, weighing 30 ± 2 g, were provided by the Experimental Animal Center of Guangxi Medical University (Guangxi, China). The research was conducted according to protocols approved by the institutional ethical committee of Guangxi Medical University (approval no.: 20110501202). All mice were housed under controlled conditions at 25 ± 2 °C, with a relative humidity of 60 ± 10%, room air changes 12–18 times/h, and a 12-h light/dark cycle. Feed and water were made available ad libitum.

After one week acclimatization, the mice were randomly divided into six groups, each consisting of 15 animals. The six groups were

designed as follows: group 1 (normal control group); group 2 (D-gal model group); group 3 (D-gal + huperzine A group); group 4 to group 6 (D-gal + PMP group). Mice in group 2 to group 6 were subcutaneously intraperitoneally (i.p.) injected with D-gal (in physiological saline) once daily at a dose of 150 mg/kg/day for 8 weeks, while mice in group 1 were treated with the same volume of physiological saline. From the third weeks, after the injection of D-gal, group 3 mice were treated with huperzine A by intragastric administration at a dose of 0.02 mg/kg/day, and group 4 to group 6 mice were orally administrated with PMP at the doses of 45, 90 and 180 mg/kg/day, respectively. At the same time, the normal control group (group 1) and the D-gal model group (group 2) mice were taken the same volume of physiological saline by intragastric administration.

At the end of the treatment period, behavioral tests were performed at the same time of the day (9:00 am to 3:00 pm). Next, the mice were euthanized by decapitation, and blood was sampled from the carotid artery, centrifuged at 3000 rpm for 10 min at 4 °C and the serum was collected. Meanwhile, the brain was rapidly excised and dissected on ice to obtain the hippocampus and the cerebral cortex. All of the serum and tissue samples were stored at −80 °C until analysis.

2.4. Open field test

The open field test was used to assess mouse locomotor activity in the different groups in order to exclude locomotor activity as an influence on memory, as described elsewhere (He et al., 2009). Locomotive activity was quantified with an open field apparatus (60 cm × 60 cm × 30 cm); the floor was divided into 25 equal squares. The animals were gently placed in the center of the arena, and behavior was recorded for 5 min. Locomotor activity was expressed as the total number of squares crossed and the total number of rearings, while emotional reactivity was expressed as the time spent in the central squares and the number of fecal boluses.

2.5. Single-trial passive avoidance test

The method used was the same as that described previously (Bagheri, Joghataei, Mohseni, & Roghani, 2011) with some modifications. The apparatus (40 cm long, 20 cm wide and 30 cm high) consisted of an illuminated chamber connected to a dark chamber by a guillotine door. Electric shocks were delivered to the grid floor by an isolated stimulator. Animals started the test in the light compartment. After a brief orientation (10 s), the gate was opened to allow the mouse to enter the darkroom. Once the mouse was inside the darkroom, the gate was closed and 0.5 mV, 1 s shocks (repeated three times with an interval of 5 s) were executed. The time that the mouse stayed in the light room was recorded. Each mouse was exposed to the test on the first, second, third and seventh day of the experiment. After shock administration, the time that the mouse hesitated before entering the darkroom again was observed. Each test was performed for no longer than 180 s.

2.6. Morris water-maze task

The Morris water-maze task was selected to evaluate spatial learning and memory (Zhang et al., 2012). The water maze was a circular pool 90 cm in diameter and 50 cm in height with a black inner surface. The tank was placed in a dimly lit soundproof room with several visual cues. The pool was divided into 4 quadrants of equal area, and filled to a depth of 30 cm with water at 20–21 °C. A black platform 6 cm in diameter and 1 cm below the surface of the water was placed in one of the quadrants. For memory acquisition (training), each mouse underwent four successive trials a day for 6 days. The interval between trials every day was 15 min to let mice recover physical capacity. The sequence of water-entering points differed each day, but the location of the platform was constant. Latency to find the platform was measured up to a maximum of 60 s. On locating the platform, the mouse was left there for 10 s prior to the next trial. If the mouse failed to locate the platform within 60 s, it was guided to the platform and allowed to stay there for 10 s. Latency and average speed to reach the platform were recorded for each trial.

The day after the last training session, mice were subjected to a probe trial session in which the platform was removed from the pool. The mice were allowed to swim for 60 s to search for it. Latency (the first time that the mice crossed the site of the removed platform), searching frequency (the number of times that the mice crossed the site of the removed platform), and the swimming time within the target quadrant were recorded and analyzed.

2.7. Biochemical assays in brain

Levels of MDA, NO, neuronal NOS (nNOS), SOD, GPX, and GSH in brain were measured using commercially available kits (Nanjing Jiancheng Bioengineering Research Institute, Nanjing, China) according to the manufacturer's instructions.

2.8. Measurement of $A\beta_{1-42}$ protein and plasticity-related proteins in hippocampus by Western blotting

The mouse hippocampi were lysed in a buffer containing 50 mM Tris–HCl (pH 6.8) containing 10% glycerol, 2% sodium dodecyl sulfate, and 5% β-mercaptoethanol. Protein lysate (50 μg) was separated by 8% SDS-PAGE and transferred onto a polyvinylidene difluoride (PVDF) membrane. After blocking in a 5% nonfat dry milk solution in washing buffer containing 10 mM Tris (pH7.5), 150 mM NaCl, and 0.05% Tween-20, the membranes were incubated overnight at 4 °C with different antibodies: rabbit polyclonal anti-β amyloid 1–42 (Abcam, UK, 1:500), rabbit monoclonal anti-PSD-95 (Thermo, USA, 1:200), rabbit polyclonal anti-phospho-NMDAR1 (Ser896) and rabbit polyclonal anti-phospho-CaMKII (Thr286) (Upstate Biotechnology, USA, 1:1000), rabbit polyclonal anti-phospho-PKA Catalytic β subunit (Ser338) (Millipore, USA, 1:1000), mouse monoclonal anti-PKCγ (Invitrogen, USA, 1:1000), mouse monoclonal anti-phospho-CREB (Ser133) (Cell Signaling Technology, USA, 1:1000), and anti-BDNF (Roche Molecular Biochemicals, Germany, 1:500). After washing three times with phosphate buffer solution, the membranes were incubated for 1.5 h with horseradish peroxidase-conjugated secondary antibody at room temperature. Following a final washing in phosphate buffer solution, the antigen-antibody staining was visualized using diaminobenzidine. Finally, the sections were washed in distilled water, dehydrated through an ethanol series, cleared with xylene and mounted in gel. The band was then scanned, and the intensity of the protein was measured using densitometry software. β-actin was used as the internal control. All values were normalized to β-actin and expressed as arbitrary units relative to the control.

2.9. Preparation of total RNA and cDNA

Total RNA was extracted from the hippocampus using Trizol reagent (Invitrogen) according to the manufacturer's instructions and stored at −70 °C. A ratio of A260/A280 in the range of 1.9–2.0 was used. The RNA concentrations were determined from the absorbances at 260 nm. Denaturing formaldehyde 1% agarose gel electrophoresis was used to check the integrity of the total RNA. cDNA was synthesized from total RNA by reverse transcriptase (Fermentas) with the primer oligo (dT) 12–18 and was stored at −20 °C.

Table 1
The primer sequences of six genes for quantitative real-time PCR.

Gene	Sense primer	Anti-sense primer
APP	5′-TTCGGACATGATTCAGGATTT-3′	5′-TGATGACAATCACGGTTGCTA-3′
BACE1	5′-AGGGCTTGCACCTGTAGGAC-3′	5′-GCCTGAGTATGACGCCAGTA-3′
CatB	5′-ACAAGCCTTCCTTCCACCCG-3′	5′-TGTCCTCACCGAACGCAACC-3′
NEP	5′-TCTTGTAAGCAGCCTCAGCC-3′	5′-CTCCCCACAGCATTCTCCAT-3′
IDE	5′-TGGTCATCTAATTGGGCACG-3′	5′-AACCTCGGGCTCCTTCCTTC-3′
GAPDH	5′-CCTTCCGTGTTCCTACCC-3′	5′-CAACCTGGTCCTCAGTGTAG-3′

2.10. Relative quantitative real-time PCR

By using the primer sequences listed in Table 1, relative quantitative real-time PCR analysis was performed with an Applied Biosystems Prism 7500 Fast Sequence Detection System. The mRNA level of amyloid protein precursor (APP), β-site amyloid cleaving enzyme-1 (BACE1), cathepsin B (CatB), neprilysin (NEP) and insulin degrading enzyme (IDE) in the hippocampus was analyzed. Mouse GAPDH gene was used as endogenous control.

SYBR® Green Real-time PCR Master Mix (TOYOBO) and iTaq™ SYBR Green Supermix with Rox (BIO-RAD) were used according to the manufacturer's instructions. The thermal cycler conditions were as follows: hold for 120 s at 95 °C, followed by three-step PCR for 40 cycles of 95 °C for 15 s, 58 °C (GAPDH, APP, BACE1 and CatB) or 60 °C (GAPDH, NEP and IDE) for 30 s, and 72 °C for 45 s. Levels of mRNA expression were determined using the 7500 Fast Real-Time PCR System SDS software version 2.0.5 (Applied Biosystems) according to the $2^{-\Delta\Delta Ct}$ method.

2.11. Assay of Ach

Ach was measured using the method of Zhong et al. (Zhong, Ge, Qu, Li, & Ma, 2009). Briefly, 0.8 ml of brain homogenate (10%, w/v) was mixed with 1.4 ml of pure water followed by addition of calabarine sulfate. Then, 0.8 ml of trichloracetic acid (1.84 M) was added and mixed. The mixture was centrifuged at 3000 rpm for 15 min, and the supernatant was removed and centrifuged at 3000 rpm for 10 min before the final supernatant was removed. Alkalinity hydroxylamine (1 ml) was added to 1.0 ml of the final supernatant and mixed. Subsequently, 0.5 ml of 4 M HCl and 0.5 ml of 0.37 M ferric chloride were added, and the mixture was shaken violently. The absorbance at 540 nm was measured. Ach levels were expressed as μg per mg of protein.

2.12. Determination of AChE activity

AChE activity in the supernatant of brain homogenate was measured according to the method of Zhong et al. (Zhong et al., 2009). Briefly, a reaction mixture that contained 470 μl of sodium phosphate (1 mM, pH 8.0), 167 μl of 2% DTNB and 33 μl of homogenate was incubated for 5 min at 37 °C. Then, 280 μl of acetylcholine iodide (2 mM) was added to the reaction mixture. After incubation for 3 min at 37 °C, the reaction was terminated by adding 50 μl of neostigmine (4 mM). The absorbance was measured at 412 nm at room temperature. AChE activity was expressed as μmol per μg of protein.

2.13. Nissl staining

Brains were fixed with 4% paraformaldehyde and cryoprotected with 30% sucrose containing phosphate-buffered saline (PBS). Serial coronal sections (15 μm) of the hippocampal regions were obtained using a rotary microtome and mounted on slides. The mounted and dried sections were rehydrated, incubated in Cresyl Violet, destained in 96% ethanol containing 0.5% acetic acid, dehydrated with isopropanol, cleared in xylene, and coverslipped. Image analysis was performed by a researcher blind to the experimental conditions. A computer-assisted light microscope (OLYMPUS, BX51) was used to scan the sections. The densities of Nissl-positive cells in the hippocampal pyramidal cell layer (CA1, CA3 and CA4) and the dentate gyrus (DG) of the scanned digital images were calculated using Image-Pro Express software (Ver 6.0). Total cell counts were averaged from both the hippocampi in 5 sections for each animal.

2.14. Histopathological examination

Brains were fixed in 4% paraformaldehyde for 48 h and then transferred to 30% sucrose in 0.1 M PBS (pH 7.4) for at least 16 h until they sank, which indicates cryoprotection. The tissues were then kept in the final sucrose solution until sectioning. Serial (neighboring) 10-μm thick sections were cut in the coronal plane and stained with hematoxylin and eosin (H&E). Histological specimens were examined by light microscopy.

2.15. Statistical analysis

Statistical analysis was performed using SPSS 11.5 for Windows. Differences between groups were assessed using a one-way analysis of variance (ANOVA) with Tukey's test for multiple post hoc comparisons. The data are presented as the means ± SE. A p-value < 0.05 was considered to be statistically significant.

3. Results and discussion

3.1. Isolation and purification of polysaccharides composition

The total yield of crude polysaccharides was 6.85% (w/w) of the dried material. To obtain high-purity and homogeneous polysaccharide products for stable and functional property, the crude polysaccharides were further purified by DEAE fast flow Sepharose anion exchange chromatography. Different fractions were selected based on total carbohydrate elution profile (Fig. 1(A)). The results showed that crude polysaccharides were mainly composed of two sub-fractions, namely CP-1and CP-2. Each fraction was eluted as a single symmetrical peak, which indicated that CP-1 (8.13%) and CP-2 (91.87%) were two homogeneous polysaccharide sub-fractions and CP-2 was the predominate fraction. To obtain high-purity and homogeneity polysaccharide products for stable functional property, the main fraction of CP-2 was further purified by Sephadex G-75 gel permeation chromatography (Fig. 1(B)). The main fraction was collected, dialyzed and lyophilized to obtain a purified polysaccharide, named as PMP.

PMP appeared as a white powder, and had a negative response to Bradford assay. No absorption at either 280 or 260 nm was detected by UV spectrophotometer. The above results showed the absence of protein and nucleic acid in PMP. Phenol–sulfuric acid assay showed PMP contained 97.82% carbohydrate. In addition, sulfate and uronic acid could not be detected in the samples of PMP.

The HPGPC (Fig. 1(C)) profiles showed a single and symmetrical sharp peak, indicating that PMP was a homogeneous polysaccharide with an average molecular weight of about

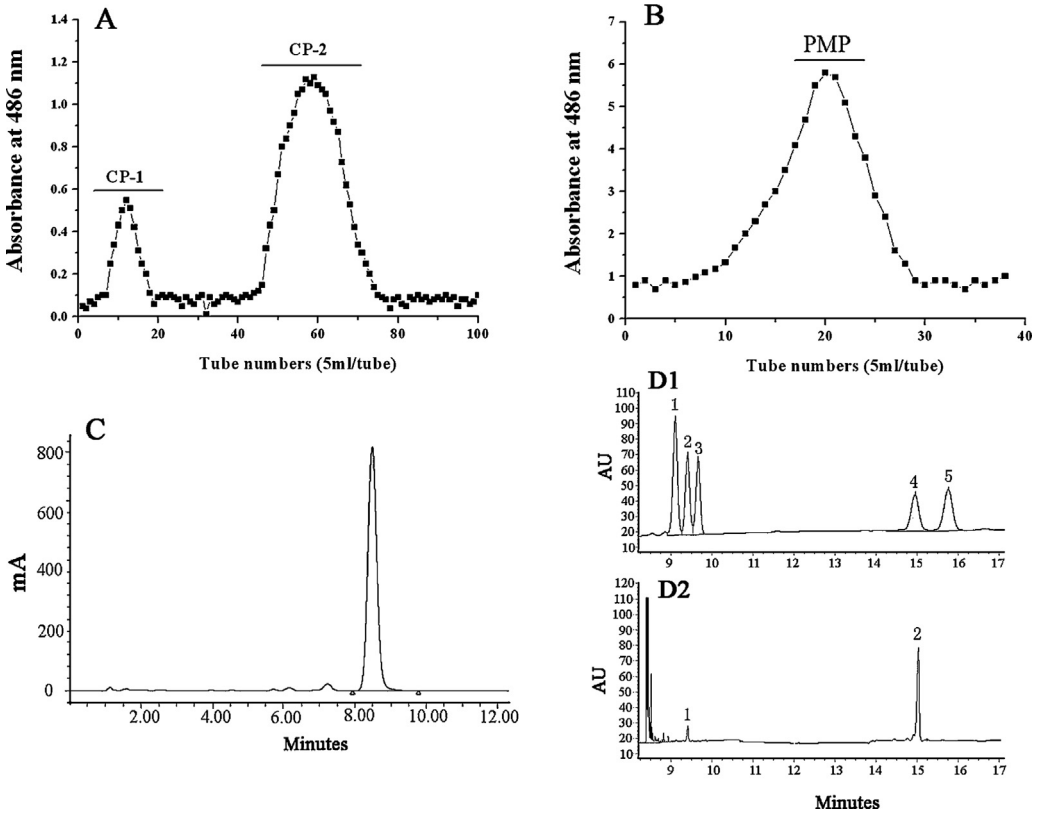

Fig. 1. Chemical analysis of PMP. (A) Elution profiles of crude polysaccharides on DEAE-Sepharose fast flow anion-exchange chromatography column (3 cm × 45 cm) with 0.1–1 M NaCl stepwise elute. (B) Profile of CP-2 on Sephadex G-75 gel permeation chromatography column (20 cm × 60 cm) with 0.1 M NaCl elute. The major fractions (i.e. 15–25 tubes) were collected, then dialyzed with water, and lyophilized to give a polysaccharide named PMP. (C) Profile of PMP in HPGPC. The sample was analyzed by a Dhpak SB 803 HQ gel filtration column (8.0 cm × 300 cm) eluted with 0.05 M Na_2SO_4, 0.5 ml/min. D: HPCE electropherogram of monosaccharides: (D1) standard mixture (Peak identity: 1: L-rhamnose, 2: D-arabinose, 3: D-xylose, 4: D-glucose and 5: D-galactose); (D2) sample (peak identity: 1: D-arabinose, 2: D-glucose).

14,301 Da, according to the calibration curve with standard dextrans.

Monosaccharide compositions of PMP were determined by the TFA hydrolysis and HPCE analysis method. The results indicated that PMP was composed of D-glucose and D-arabinose with molar percent of 90.79% and 9.21%, respectively (Fig. 1(D)).

3.2. The effects of PMP on locomotor activity and emotional reactivity in the open field test

As a measure of general locomotor activity as well as anxiety, mice were examined in an open field chamber. The number of crossings, rearings and fecal boluses and the time in the central squares were recorded. As shown in Fig. 2(A), the number of rearings and fecal boluses in the normal mice were significantly lower than in the D-gal model control mice; locomotor activities of mice in all other groups did not differ.

3.3. Passive avoidance test

As shown in Fig. 2(B), the passive avoidance time in the D-gal model control group was significantly shorter than in the normal control group. However, the passive avoidance times of mice supplemented with 90 or 180 mg/kg PMP or 0.02 mg/kg huperzine A were longer than those of the D-gal model control mice.

3.4. The effects of PMP on spatial learning and memory deficits

Mice were trained in the water maze for 6 days. Normal control mice rapidly learned the location of the platform, but D-gal model control mice had significantly longer escape latencies on every test day. Treating mice with 90 or 180 mg/kg PMP or 0.02 mg/kg huperzine A resulted in a significant decrease in escape latency (Fig. 2(C)).

In the probe test, latency (the first time that the mice crossed the site of the removed platform) was increased and searching frequency (the number of times that the mice crossed the site of the removed platform) was decreased in D-gal model control mice compared to normal control mice. The latency was decreased by PMP or huperzine A administration, and searching frequency was increased significantly by administration of 90 and 180 mg/kg PMP. In addition, treatment with PMP or huperzine A increased the swimming time within the target quadrant (Fig. 2(D)).

3.5. Biochemical assays

Although the exact molecular basis of aging remains uncertain, accumulated knowledge suggests that it may be related to an increase in free radicals (Burke & Barnes, 2006; Kishida & Klann, 2007). According to the Free Radical Theory of Aging, the generation of reactive oxygen species (ROS) and/or free radical-induced oxidative stress can lead to cell and tissue damage, paralleled by alterations in the function of the genetic apparatus, thus resulting in aging and age-related memory loss (Muller, Lustgarten, Jang, Richardson, & Van Remmen, 2007). Many studies have shown that aging and particularly brain aging are associated with the action of free radicals and their intermediate products, such as MDA, NO, etc. Cells can defend themselves against the harmful effects of free radicals with adequate protective mechanisms: SOD, GSH, GPx, etc. (Devasagayam et al., 2004). There is a balance that exists

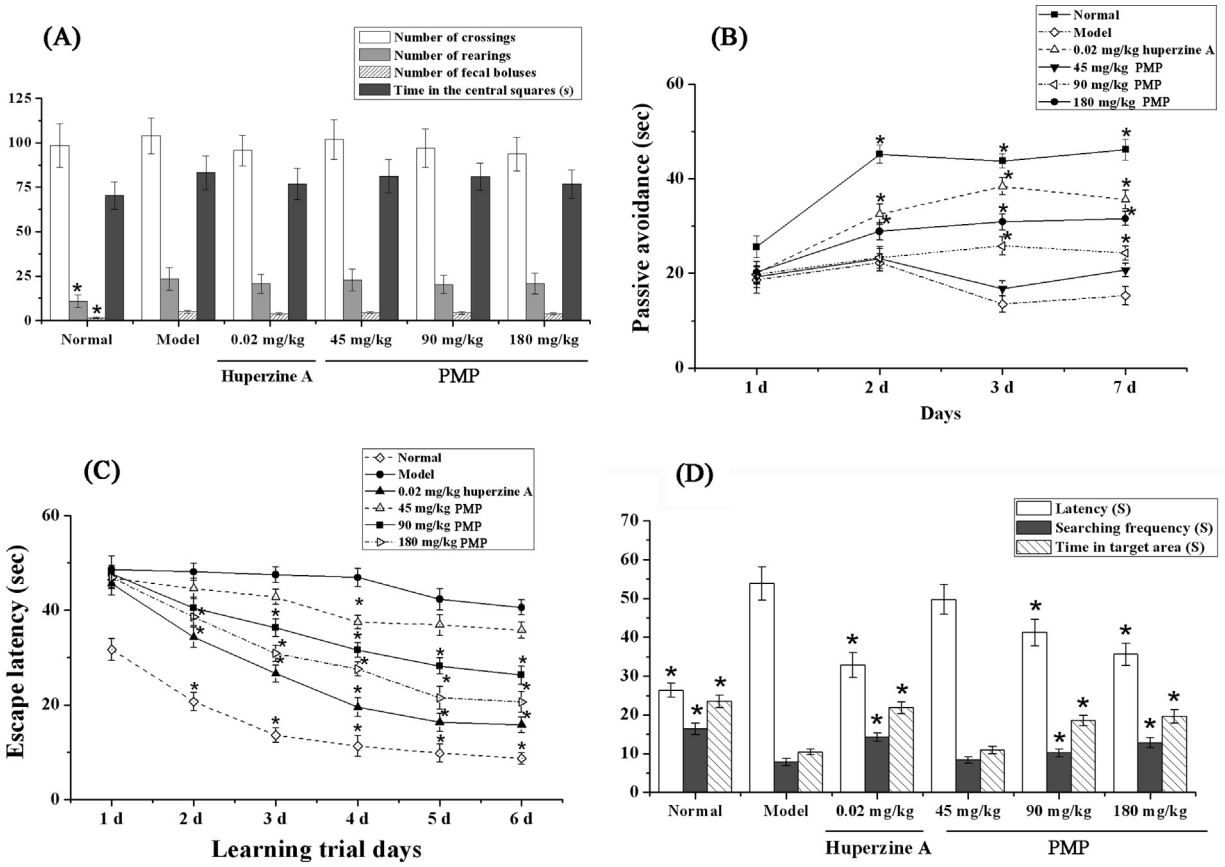

Fig. 2. Behavioral tests. (A) The locomotor behavior and emotional reactivity of mice in the open field test. Locomotive activities of mice in the 3 dose PMP treated groups were no different from D-gal model control mice. (B) The effects of PMP on the learning and memory impairment in the passive avoidance test. Avoidance tests were performed for three consecutive days as well as on the seventh day of the study. (C) The training trial sessions. Spatial learning and memory ability of D-gal model control mice was impaired all throughout the test; and the impairment was improved by the administration of different dosages PMP. (D) The probe trial session. Latency: the first time that the mice crossed the former platform; searching frequency: the number of times that the mice crossed the site of the removed platform; time in target area: the swimming time within the target quadrant. Data values are expressed as means ± SE, $^{*}P < 0.05$ vs. D-gal model control.

between free radicals and antioxidants under normal physiological conditions in healthy people and in other organisms. However, in the process of aging, the balance is broken; free radical generation may increase and antioxidant defense systems may gradually diminish in efficacy (Reiter, 1995; Reiter, Acuña-Castroviejo, Tan, & Burkhardt, 2001). In the present study, levels of MDA, NO, neuronal NOS (nNOS), SOD, GSH and GPX in brain were detected. As shown in Fig. 4, MDA, NO and nNOS content was significantly higher in D-gal model control mice when compared with normal control mice. Administration of PMP at 90 and 180 mg/kg body weight significantly decreased the MDA, NO and nNOS levels (Fig. 3(A)). In addition, the SOD, GSH and GPX activities were significantly lower in the D-gal model control mice when compared with the normal control mice. However, the mice treated with PMP showed a significant improvement toward the normal value (Fig. 3(B)). These results indicate that PMP treatment significantly enhances the antioxidant defense systems and alleviates the harmful effects of free radicals.

3.6. The effect of PMP on $A\beta_{1-42}$ protein in hippocampus

Aggregation and deposition of Aβ in the brain is a key step in the pathogenesis of AD that elicits a cascade of cellular events leading ultimately to neuronal loss and dementia (Hardy & Selkoe, 2002). As shown in Fig. 4(A) and (B), the content of Aβ in the hippocampus of D-gal-induced model mice was significantly higher than in the normal control. Administration of PMP significantly decreased the Aβ content, and this decrease may be one of the mechanisms of action of PMP in ameliorating cognition degeneration in mice.

3.7. Effects of PMP on the expression of genes related to Aβ

An imbalance between the production of Aβ and its removal causes Aβ accumulation. Aβ is produced by proteolytic processing of APP. Proteases referred to as β-secretase and γ-secretase cleave at the N- and C-termini of Aβ within APP to generate Aβ. Aβ then undergoes secretion to provide extracellular Aβ that produces neurotoxic effects, with aggregation and accumulation in amyloid plaques of AD brains. BACE1 and CatB are generally considered to be the critical β-secretases (Haque, Banik, & Ray, 2008; Hook, Schechter, Demuth, & Hook, 2008; Stockley & O'Neill, 2008). Additionally, several enzymes within the central nervous system are capable of degrading Aβ. Among these enzymes, there is increasing evidence that NEP and IDE are primarily responsible for degrading Aβ in the brain (Chen et al., 2010). Therefore, five genes associated with the Aβ pathway, APP, BACE1, CatB, NEP and IDE, were analyzed to explore the molecular mechanism of the effect of PMP on abnormal Aβ levels. Statistical analysis showed higher APP, BACE1 and CatB levels and significantly lower NEP and IDE levels in the D-gal model control group compared with the normal control group. Treatment with PMP induced changes in the mRNA levels: APP, BACE1 and CatB mRNA levels were decreased and NEP and IDE mRNA levels were markedly increased after treatment (Fig. 4(C)). This indicates that PMP may lower Aβ content by modulating the

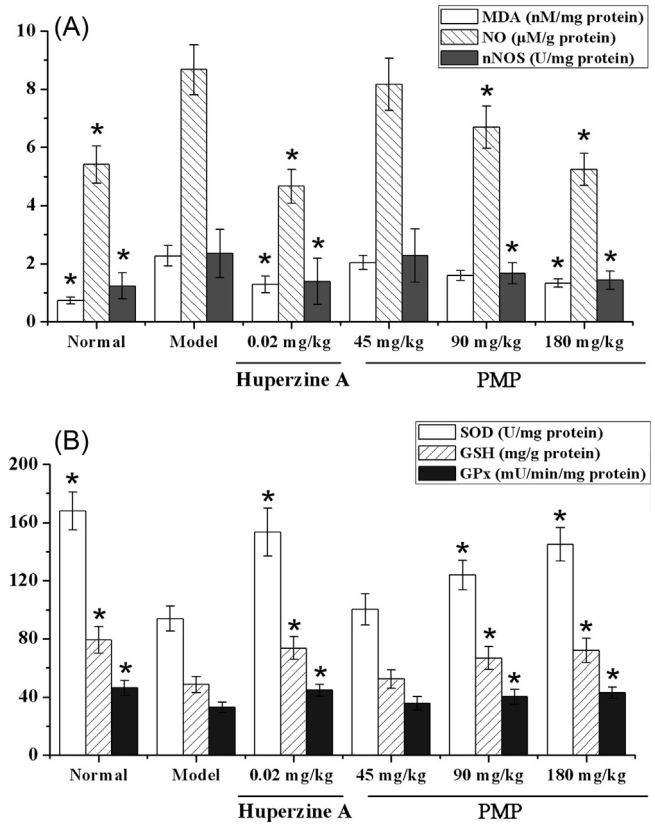

Fig. 3. The effects of PMP on brain levels of MDA, NO, nNOS, SOD, GPX and GSH. Data values are expressed as means ± SE, $^{*}P < 0.05$ vs. D-gal model control.

Aβ pathway (particularly inducing a decline in the levels of APP, BACE1 and CatB and a rise in the levels of NEP and IDE).

3.8. The effects of PMP on the expression of synapse plasticity-related proteins in the hippocampus

Initially, the decline of memory function with age is believed to be due to changes in synaptic function rather than a loss of neurons (Lesné et al., 2006). Postsynaptic density 95 (PSD-95), highly abundant at the postsynaptic density and a major constituent of dendritic spines, can be regarded as a key molecule in neuronal information storage-related processes (Bevilaqua, Medina, Izquierdo, & Cammarota, 2005). The processes of learning, memory formation and functional plasticity, such as long-term potentiation (LTP), are associated with the phosphorylation state of N-methyl-D-aspartic acid receptors (NMDARs) and Ca^{2+}/calmodulin-dependent protein kinase II (CaMKII) (Ahmed & Frey, 2005). NMDA receptor subunit 1 (NMDAR1) is a subunit required for functional receptor formation (Lau, Saha, Faris, & Russek, 2004). A previous study reported impaired learning and memory in rats in which the NMDAR1 subunit was knocked down in a subset of hippocampal neurons (Cheli et al., 2006). CaMKII, acting through its autophosphorylation properties, is thought to represent a "molecular switch" for the transition from short-term to long-term information storage (Vaynman, Ying, & Gomez-Pinilla, 2007). There is strong evidence that the protein kinase C (PKC) and protein kinase A (PKA) signaling pathways, especially those of isoenzyme-PKA Cβ and PKCγ, regulate important molecular events in learning and memory processes and in the neurodegenerative pathophysiology of AD (Pang & Lu, 2004). In addition, cAMP-response element binding protein (CREB) has been identified as a key molecule initiating the transcriptional activation of other genes encoding proteins that presumably play an important role in the structural and functional changes underlying information storage (Lamprecht, 1999). Indeed, CREB activation through its phosphorylation on Serine-133 (p-CREB) controls the induction of regulatory immediate-early genes whose products subsequently induce the transcription of late downstream genes and activate direct "effector" proteins, such as structural proteins, signaling enzymes or growth factors that are essential for long-term memory. Brain-derived neurotrophic factor (BDNF) is a powerful modulator of neuronal excitability and synaptic transmission and plays a role in hippocampal-dependent learning and memory (Bimonte, Nelson, & Granholm, 2003; Gómez-Pinilla et al., 2007). In this study, the expression of the above mentioned synaptic plasticity related proteins were evaluated. As shown in Fig. 5, significantly lower expression of these proteins was observed in the D-gal model control group when compared with the normal control. Animals treated with PMP exhibited a significant increase in the expression of these proteins. This result suggests that the protective effect of PMP on the intact of synapse in hippocampus may be a neurobiological basis for improving cognition deterioration.

3.9. Ach level and AChE activity in brain

The cholinergic system has been implicated in several neuropsychic functions, such as learning, memory, sleep, etc. (Everitt

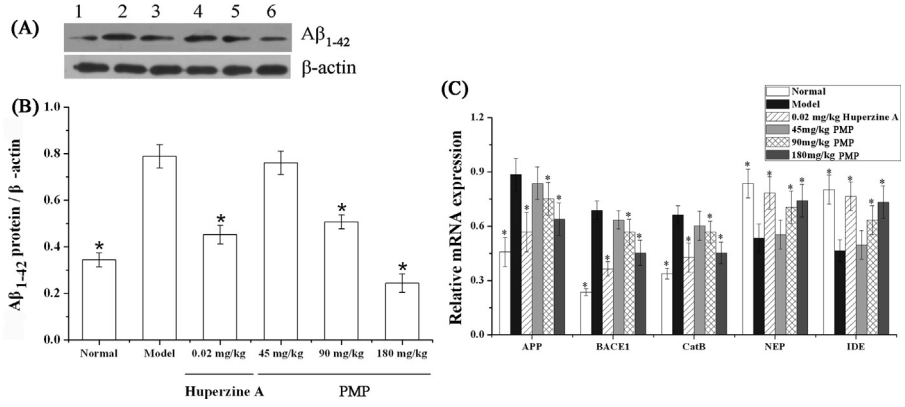

Fig. 4. The effects of PMP on $Aβ_{1-42}$ protein and expression of genes related to Aβ. (A) The bands are a representative of the blot. Lane 1, normal control group; lane 2, D-gal model control group; lane 3, 0.02 mg/kg huperzine A-treated group; lane 4–6, 45, 90 and 180 mg/kg PMP-treated groups. 50 μg protein lysate was separated by 8% SDS-PAGE in Western blotting. (B) Relative protein level between the tested target protein and internal standard β-actin band was calculated and labeled on *Y* axis. (C) APP, BACE1, CatB, NEP and IDE mRNA expression were assayed by real-time PCR in the hippocampus. APP: amyloid protein precursor; BACE1: β-site amyloid cleave enzyme-1; CatB: cathepsin B; NEP: neprilysin; IDE: insulin degrading enzyme. Data values are expressed as means ± SE, $^{*}P < 0.05$ vs. D-gal model control.

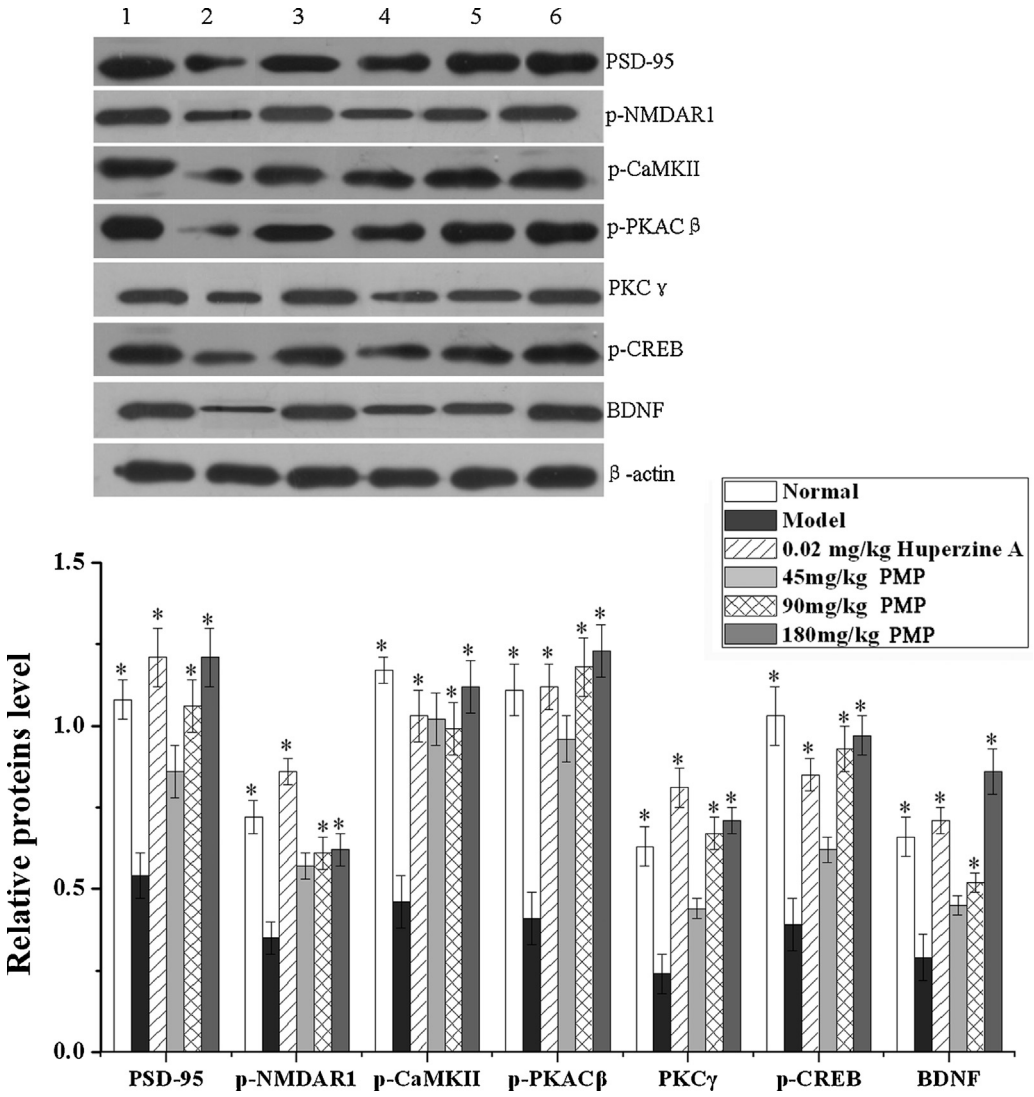

Fig. 5. The effects of PMP on the expressions of synapse plasticity-related proteins in hippocampus. (A) The bands are a representative of the blot. Lane 1, normal control group; lane 2, D-gal model control group; lane 3, 0.02 mg/kg huperzine A-treated group; lane 4–6, 45, 90 and 180 mg/kg PMP-treated groups. (B) Relative protein level between the tested target protein and internal standard β-actin band was calculated and labeled on *Y* axis. Data values are expressed as means ± SE, $^{*}P < 0.05$ vs. D-gal model control.

& Robbins, 1997). Ach plays a principal role in modulating these functions (Mohapel, Leanza, Kokaia, & Lindvall, 2005); AChE is responsible for the degradation of Ach to acetate and choline in the synaptic cleft. As shown in Fig. 6, AChE activity was significantly higher in D-gal-induced model mice. As a consequence of the increase of AChE activity, the Ach level was lower in D-gal-induced model mice. Treatment with 180 mg/kg PMP reversed the abnormalities in Ach level and AChE activity. This result suggests that PMP may improve dysfunction of the cholinergic system.

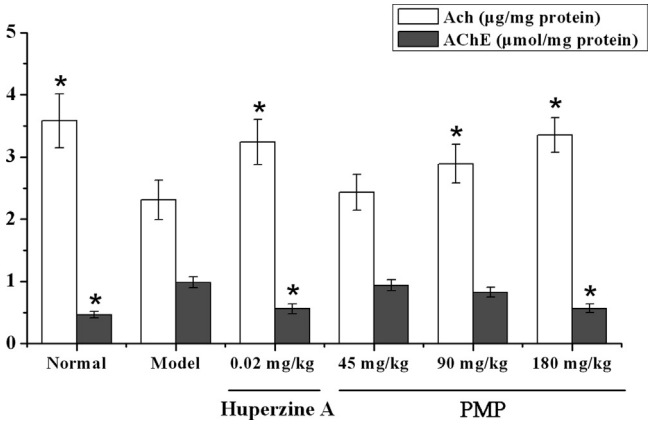

Fig. 6. The effects of PMP on Ach level and the AChE activity of mice brains. Data values are expressed as means ± SE, $^{*}P < 0.05$ vs. D-gal model control.

3.10. The effect of PMP on Nissl-positive cell density in the hippocampus

After Nissl staining, intact cells were smoothly stained a light blue color with regularly shaped cell bodies and a large centrally located nucleus. As shown in Fig. 7(A), the Nissl positive cell numbers per mm^2 of the CA1 and CA3 regions of the hippocampus showed no significant differences among all groups. The cell density of the granule neurons in dentate gyrus (DG) was significantly lower in D-gal model control mice compared with normal mice,

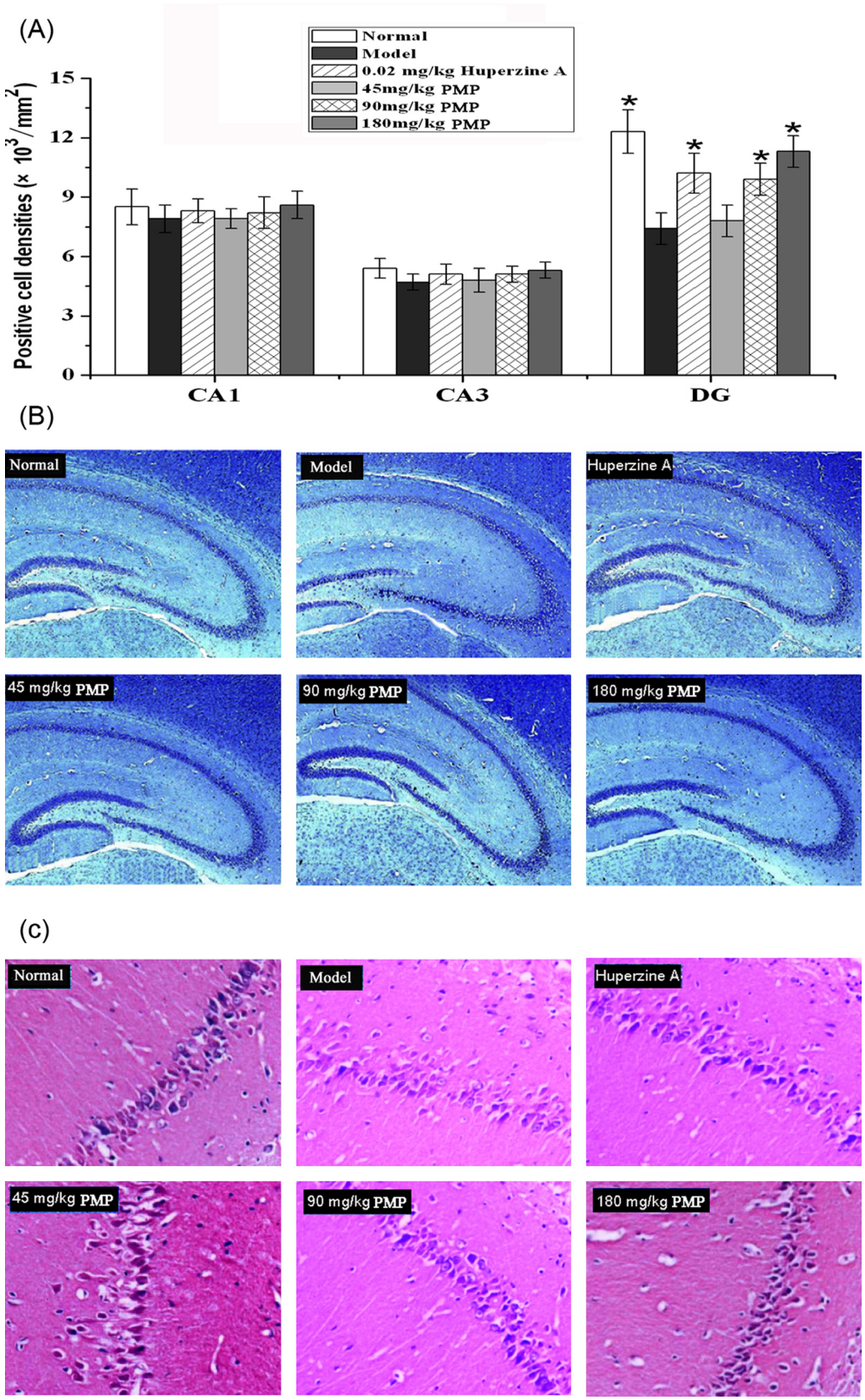

Fig. 7. The effects of PMP on Nissl-positive cell densities and histopathological changes. (A) Nissl-positive cell densities (positive cells per mm^2) in the CA1, CA3 and DG of hippocampus. Data values are expressed as means ± SE, $^*P < 0.05$ vs. D-gal model control. (B) Normal control showed intact and well-arranged neurons; in contrast, neurons of D-gal model control showed reduced staining, and they were significantly swollen and arranged abnormally. Administration of PMP or huperzine A diminished the loss and swelling of neurons in the hippocampus, and neurons recovered their characteristic shape and arrangement. (C) Representative photomicrograph showing the histology of CA1 hippocampal neurons (H&E, 400×).

and administration of PMP significantly prevented cell loss in the hippocampus.

In the DG of D-gal model control mice, neuronal loss was accompanied by swollen neurons and an abnormal neuronal arrangement. In contrast, neurons in the other groups were intact and well-arranged (Fig. 7(B)).

3.11. Histopathological findings

As shown in Fig. 7(C), the neurons in the normal control group were large, conical shaped cells with well delineated amphophilic cytoplasm and round vesicular nuclei with prominent nucleoli. In the D-gal model control group, the CA1 layer neurons showed pronounced shrinkage of the neuronal bodies with the nuclei losing their regular outlines and becoming hyperchromatic. The shrinkage of the cells also caused a clear space to form around each neuron. Treatment with huperzine A or PMP significantly attenuated the shrinkage of the neurons and decreased the retraction space around the neurons.

4. Conclusions

Our study demonstrated that PMP significantly improved cognitive impairment and neuropathologic lesions induced by D-gal in mice, and these effects may be mediated by scavenging free radicals, modulating the activity of antioxidant enzymes, decreasing the content and deposition of Aβ, improving the dysfunction of synaptic plasticity, reversing the abnormality of Ach level and AChE activity, and protecting hippocampal neurons from damage. These data suggest that PMP is helpful in preventing age-related cognitive deficits.

Acknowledgments

This work was supported by the National Natural Science Foundation of China (No. 30960504), Guangxi Natural Science Foundation Major Project (No. 2011GXNSFD018030) and Nanning Tackle Hard-Nut Problems in Science and Technology and Trial Production of New Products (No. 201102084C).

References

Ahmed, T., & Frey, J. U. (2005). Plasticity-specific phosphorylation of CaMKII, MAP-kinases and CREB during late-LTP in rat hippocampal slices in vitro. *Neuropharmacology*, *49*(4), 477–492.

Bagheri, M., Joghataei, M., Mohseni, S., & Roghani, M. (2011). Genistein ameliorates learning and memory deficits in amyloid β_{1-40} rat model of Alzheimer's disease. *Neurobiology of Learning and Memory*, *95*(3), 270–276.

Bevilaqua, L., Medina, J., Izquierdo, I., & Cammarota, M. (2005). Memory consolidation induces N-methyl-D-aspartic acid-receptor-and Ca^{2+}/calmodulin-dependent protein kinase II-dependent modifications in alpha-amino-3-hydroxy-5-methylisoxazole-4-propionic acid receptor properties. *Neuroscience*, *136*(2), 397–403.

Bimonte, H. A., Nelson, M. E., & Granholm, A. C. E. (2003). Age-related deficits as working memory load increases: Relationships with growth factors. *Neurobiology of Aging*, *24*(1), 37–48.

Bradford, M. M. (1976). A rapid and sensitive method for the quantitation of microgram quantities of protein utilizing the principle of protein–dye binding. *Analytical Biochemistry*, *72*(1), 248–254.

Burke, S. N., & Barnes, C. A. (2006). Neural plasticity in the ageing brain. *Nature Reviews Neuroscience*, *7*(1), 30–40.

Castegna, A., Aksenov, M., Aksenova, M., Thongboonkerd, V., Klein, J. B., Pierce, W. M., et al. (2002). Proteomic identification of oxidatively modified proteins in Alzheimer's disease brain. Part I: Creatine kinase BB, glutamine synthase, and ubiquitin carboxy-terminal hydrolase L-1. *Free Radical Biology and Medicine*, *33*(4), 562–571.

Cheli, V., Adrover, M., Blanco, C., Ferrari, C., Cornea, A., Pitossi, F., et al. (2006). Knocking-down the NMDAR1 subunit in a limited amount of neurons in the rat hippocampus impairs learning. *Journal of Neurochemistry*, *97*(s1), 68L 73.

Chen, P. T., Liao, T. Y., Hu, C. J., Wu, S. T., Wang, S. S., & Chen, R. P. (2010). A highly sensitive peptide substrate for detecting two Ass-degrading enzymes: Neprilysin and insulin-degrading enzyme. *Journal of Neuroscience Methods*, *190*(1), 57–62.

Cui, X., Zuo, P., Zhang, Q., Li, X., Hu, Y., Long, J., et al. (2006). Chronic systemic D-galactose exposure induces memory loss, neurodegeneration, and oxidative damage in mice: Protective effects of R-α-lipoic acid. *Journal of Neuroscience Research*, *83*(8), 1584–1590.

De Iuliis, A., Grigoletto, J., Recchia, A., Giusti, P., & Arslan, P. (2005). A proteomic approach in the study of an animal model of Parkinson's disease. *Clinica Chimica Acta*, *357*(2), 202–209.

Devasagayam, T., Tilak, J., Boloor, K., Sane, K., Ghaskadbi, S., & Lele, R. (2004). Free radicals and antioxidants in human health: Current status and future prospects. *Journal of The Association of Physicians of India*, *52*, 794–804.

Everitt, B. J., & Robbins, T. W. (1997). Central cholinergic systems and cognition. *Annual Review of Psychology*, *48*(1), 649–684.

Filisetti-Cozzi, T. M., & Carpita, N. C. (1991). Measurement of uronic acids without interference from neutral sugars. *Analytical Biochemistry*, *197*(1), 157–162.

Gómez-Pinilla, F., Huie, J., Ying, Z., Ferguson, A., Crown, E., Baumbauer, K., et al. (2007). BDNF and learning: Evidence that instrumental training promotes learning within the spinal cord by up-regulating BDNF expression. *Neuroscience*, *148*(4), 893–906.

Haque, A., Banik, N. L., & Ray, S. K. (2008). New Insights into the roles of endolysosomal cathepsins in the pathogenesis of Alzheimers disease: Cathepsin inhibitors as potential therapeutics. *CNS and Neurological Disorders – Drug Targets*, *7*(3), 270–277.

Hardy, J., & Selkoe, D. J. (2002). The amyloid hypothesis of Alzheimer's disease: Progress and problems on the road to therapeutics. *Science*, *297*(5580), 353–356.

He, J., Luo, H., Yan, B., Yu, Y., Wang, H., Wei, Z., et al. (2009). Beneficial effects of quetiapine in a transgenic mouse model of Alzheimer's disease. *Neurobiology of Aging*, *30*(8), 1205–1216.

Hook, V., Schechter, I., Demuth, H. U., & Hook, G. (2008). Alternative pathways for production of β-amyloid peptides of Alzheimer's disease. *Biological Chemistry*, *389*(8), 993–1006.

Huang, Z. S., Jiao, Y., Zhang, S. J., & Huang, R. B. (2008). Improvement of LYSP on learning and memory abilities in the elderly aging SAMP8 mice model. *Chinese Journal of Gerontology*, *11*(28), 2086–2088.

Huang, Z. S., Lin, X., Zhang, S. J., Jiao, Y., Jiang, W. Z., & Huang, R. B. (2008). Effects of LYS polysaccharides on learning and memory as well as monoamine neurotransmitter content in SAMP8 mice's brain. *China Pharmacy*, *19*(9), 647–649.

Huang, Z. S., Xie, H. Y., Zhang, S. J., Jiao, Y., Jiang, W. Z., & Huang, R. B. (2008). Effects of Longyanshen polysaccharides on free radical metabolism in senescence accelerated-prone mice. *Neural Regeneration Research*, *3*(10), 1099–1102.

Huang, Z. S., Zhang, S. J., Xie, H. Y., Lin, X., Jiang, W. Z., & Huang, R. B. (2009). Key gene and protein changes in the beta-amyloid pathway following Longyanshen polysaccharides treatment in a mouse model of Alzheimer's disease. *Neural Regeneration Research*, *4*(10), 756–762.

Kawai, Y., Seno, N., & Anno, K. (1969). A modified method for chondrosulfatase assay. *Analytical Biochemistry*, *32*(2), 314–321.

Kishida, K. T., & Klann, E. (2007). Sources and targets of reactive oxygen species in synaptic plasticity and memory. *Antioxidants and Redox Signaling*, *9*(2), 233–244.

Lamprecht, R. (1999). CREB: A message to remember. *Cellular and Molecular Life Sciences(CMLS)*, *55*(4), 554–563.

Lau, G. C., Saha, S., Faris, R., & Russek, S. J. (2004). Up-regulation of NMDAR1 subunit gene expression in cortical neurons via a PKA-dependent pathway. *Journal of Neurochemistry*, *88*(3), 564–575.

Lesné, S., Koh, M. T., Kotilinek, L., Kayed, R., Glabe, C. G., Yang, A., et al. (2006). A specific amyloid-β protein assembly in the brain impairs memory. *Nature*, *440*(7082), 352–357.

Li, L. (2011). Research Progress in *Millettia pulchra*. *Modern Chinese Medicine*, *13*(12), 53–55.

Mohapel, P., Leanza, G., Kokaia, M., & Lindvall, O. (2005). Forebrain acetylcholine regulates adult hippocampal neurogenesis and learning. *Neurobiology of Aging*, *26*(6), 939–946.

Muller, F. L., Lustgarten, M. S., Jang, Y., Richardson, A., & Van Remmen, H. (2007). Trends in oxidative aging theories. *Free Radical Biology and Medicine*, *43*(4), 477–503.

Pang, P. T., & Lu, B. (2004). Regulation of late-phase LTP and long-term memory in normal and aging hippocampus: Role of secreted proteins tPA and BDNF. *Ageing Research Reviews*, *3*(4), 407–430.

Reiter, R. J. (1995). Oxidative processes and antioxidative defense mechanisms in the aging brain. *The FASEB Journal*, *9*(7), 526–533.

Reiter, R. J., Acuña-Castroviejo, D., Tan, D. X., & Burkhardt, S. (2001). Free radical-mediated molecular damage. *Annals of the New York Academy of Sciences*, *939*(1), 200–215.

Stockley, J., & O'Neill, C. (2008). Understanding BACE1: Essential protease for amyloid-β production in Alzheimer's disease. *Cellular and Molecular Life Sciences*, *65*(20), 3265–3289.

Taylor, K. A. (1995). A modification of the phenol/sulfuric acid assay for total carbohydrates giving more comparable absorbances. *Applied Biochemistry and Biotechnology*, *53*(3), 207–214.

Vaynman, S., Ying, Z., & Gomez-Pinilla, F. (2007). The select action of hippocampal calcium calmodulin protein kinase II in mediating exercise-enhanced cognitive function. *Neuroscience*, *144*(3), 825–833.

Wei, H., Li, L., Song, Q., Ai, H., Chu, J., & Li, W. (2005). Behavioural study of the D-galactose induced aging model in C57BL/6J mice. *Behavioural Brain Research*, *157*(2), 245–251.

Zhang, Q., Li, X., Cui, X., & Zuo, P. (2005). D-Galactose injured neurogenesis in the hippocampus of adult mice. *Neurological Research*, *27*(5), 552–556.

Zhang, X., Wang, J., Xing, Y., Gong, L., Li, H., Wu, Z., et al. (2012). Effects of ginsenoside Rg1 or 17β-estradiol on a cognitively impaired, ovariectomized rat model of Alzheimer's disease. *Neuroscience*, *220*, 191–200.

Zhang, X. L., Jiang, B., Li, Z. B., Hao, S., & An, L. J. (2007). Catalpol ameliorates cognition deficits and attenuates oxidative damage in the brain of senescent mice induced by D-galactose. *Pharmacology Biochemistry and Behavior*, *88*(1), 64–72.

Zhong, S. Z., Ge, Q. H., Qu, R., Li, Q., & Ma, S. P. (2009). Paeonol attenuates neurotoxicity and ameliorates cognitive impairment induced by D-galactose in ICR mice. *Journal of the Neurological Sciences*, *277*(1), 58–64.